

The Effect of pH on the Dimensionality of Coordination Polymers

Long Pan, Thomas Frydel, Michelle B. Sander, Xiaoying Huang, and Jing Li*

Department of Chemistry, Rutgers University, Camden, New Jersey 08102

Received September 6, 2000

Hydrothermal reactions of simple alkaline salts or their hydroxides with 3,5-pyrazoledicarboxylic acid (H₃pdc) yielded seven new compounds. At a lower pH level three one-dimensional structures [Ca(Hpdc)(H₂O)₄]·2H₂O (**1**), [Ca(Hpdc)(H₂O)₄]·H₂O (**2**), and [Ba(H₂pdc)₂(H₂O)₄]·2H₂O (**6**) were obtained by evaporation of the solutions resulting from hydro(solvo)thermal reactions of MCl₂ (M = Ca, Ba) with H₃pdc in water (**1**, **6**) or in water/Et₃N (**2**) at 150 °C for 3 days. Crystal structures of **1** and **2** contain zigzag chains of metal centers bridged by a single Hpdc²⁻ ligand, whereas structure **6** consists of linear chains of metal centers bridged by two H₂pdc⁻ ligands. A dimer molecule [Sr(H₃pdc)(H₂pdc)₂(H₂O)₃]₂·2(H₃pdc)·4H₂O (**4**) was obtained from a similar hydrothermal reaction using Sr(ClO₄)₂·6H₂O instead of MCl₂. This compound contains [2+2] metallomacrocycles. At higher pH levels (pH = 4–6), the three-dimensional polymers [M(Hpdc)(H₂O)] (Ca **3**, Sr **5**, Ba **7**) were isolated by reactions of MCl₂ (M = Ca, Sr, Ba) with H₃pdc in water/Et₃N or in M(OH)₂ (M = Ca, Sr, Ba) with H₃pdc in water under hydro(solvo)thermal conditions (150 °C, 3 days). Calcium and strontium are seven- and nine-coordinated in **3** and **5**, respectively; barium is nine- and ten-coordinated in **7**. It was observed that the increase in pH resulted in a higher connectivity level of ligands, which in turn leads to a higher dimensionality of the crystal structures. The correlation between the structures and pH values will be discussed. Crystal data: for **1**, monoclinic, space group *P*2₁/*n* (No. 14), with *a* = 8.382(2), *b* = 12.621(3), *c* = 11.767(2) Å, β = 98.91(3)°, *Z* = 4; for **2**, **3**, and **5**, monoclinic, space group *P*2₁/*c* (No. 14), *Z* = 4, *a* = 7.711(2), *b* = 15.574(3), *c* = 9.341(2) Å, β = 96.73(3)°, *Z* = 4 (**2**), *a* = 6.616(1), *b* = 12.654(3), *c* = 8.782(2) Å, β = 103.65(3)°, *Z* = 4 (**3**), *a* = 9.213(2), *b* = 12.088(3), *c* = 6.196(2) Å, β = 98.96(3)° (**5**); for **4** and **7**, triclinic, space group *P* $\bar{1}$ (No. 2), with *a* = 11.263(2), *b* = 11.460(3), *c* = 12.904(2) Å, α = 71.54(3), β = 98.96(3), γ = 89.03(3)°, *Z* = 1 (**4**), *a* = 7.107(1), *b* = 9.780(2), *c* = 11.431(2) Å, α = 74.69(3), β = 73.39(3), γ = 85.29(3)°, *Z* = 2 (**7**); for **6**, monoclinic, space group *C*2/*c* (No. 15), with *a* = 20.493(4), *b* = 6.708(1), *c* = 15.939(3) Å, β = 123.56(3)°, *Z* = 4.

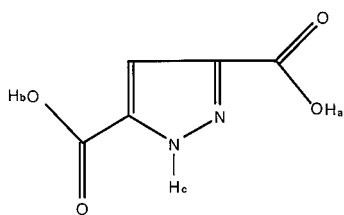
Introduction

Synthesis and characterization of coordination polymers is an area of substantial interest due to the formation of fascinating structures with potentials in applications.¹ High dimensional coordination polymers often exhibit important functionality that low dimensional structures are lacking. For example, porosity in a homochiral framework structure allows for enantioselective separation and catalysis.² Three-dimensional magnetic networks with porosity may possess both useful magnetic properties³ and zeolite-like behavior,⁴ which would further enhance the functionality and performance of these materials. While interest in this area has grown exponentially, chemists are often plagued with at least two complex problems in designing compounds with high dimensionality structures. First, how to overcome the difficulties of lattice interpenetration, which usually reduce the effective volume. Second, what can be done to prevent the ancillary ligands, such as water or other solvents, from occupying the metal coordination sites. One way that proves to be effective in preventing the structures from interpenetration is to use super-tetrahedral clusters or bimetallic tetracarboxylate units as building blocks to fabricate porous metal-organic frameworks.⁵ As for the second problem, coordination of a terminal ligand can sometimes be avoided through high reaction temperatures and high pH values in the reactions.⁶ Recently, we have exploited the effect of pH on the structure dimensionality. Our studies^{6b–c} based on H₃pdc have shown that a reaction

product is directly affected by the acidity level of a solution. As shown in Scheme 1, H₃pdc contains three different hydrogens

- (1) Long D.-L.; Blake, A. J.; Champness, N. R.; Schröder, M. *Chem. Commun.* **2000**, 1369. (b) Glake, A. J.; Champness, N. R.; Khlobystov, A.; Lemenovskii, D. A.; Li, W.-S.; Schröder, M. *Chem. Commun.* **1997**, 2027. (c) Carlucci, L.; Ciani, G.; Proserpio, D. M. *Chem. Commun.* **1999**, 49. (d) Carlucci, L.; Ciano, G.; Moret, M.; Proserpio, D. M.; Rizzato, S. *Angew. Chem., Int. Ed.* **2000**, *39*, 1506. (e) Abrahams, B. F.; Batten, S. R.; Grannas, M. J.; Hamit, H.; Hoskins, B. F.; Robson, R. *Angew. Chem., Int. Ed.* **1999**, *38*, 1475. (f) Abrahams, B. F.; Jackson, P. A.; Robson, R. *Angew. Chem., Int. Ed.* **1998**, *37*, 2656. (g) Biradha, K.; Domasevitch, K. V.; Moulton, B.; Seward, C.; Zaworotko, M. J. *Chem. Commun.* **1999**, 1327. (h) Biradha, K.; Seward, C.; Zaworotko, M. J. *Angew. Chem., Int. Ed.* **1999**, *38*, 492. (i) Tong, M.-L.; Chen, X.-M.; Ye, B.-H.; Ji, L.-N. *Angew. Chem., Int. Ed.* **1999**, *38*, 2237. (j) Choi, H. J.; Suh, M. P. *J. Am. Chem. Soc.* **1998**, *120*, 10622. (k) Lin, K. J.; *Angew. Chem., Int. Ed.* **1999**, *38*, 2730. (l) Reineke, T. M.; Eddaoudi, M.; Fehr, M.; Kelley, D.; Yaghi, O. M. *J. Am. Chem. Soc.* **1999**, *121*, 1651. (m) Zhang, H.; Wang, X.; Teo, B. K. *J. Am. Chem. Soc.* **1996**, *118*, 11813. (n) Lin W.; Evans, O. R.; Xiong, R.-G.; Wang, Z.; Wong, G. K. *Angew. Chem., Int. Ed.* **1999**, *38*, 536. (o) Miller, S. A.; Kim, E.; Grau, D. H.; Gin, D. L. *Angew. Chem., Int. Ed.* **1999**, *38*, 3022. (p) Fujita, M.; Kwon, Y. J.; Washizu, S.; Ogura, K. *J. Am. Chem. Soc.* **1994**, *116*, 1151. (q) Zhao, H.; Heintz, R. A.; Ouyang, X.; Dunbar, K. R.; Campana, C. F.; Rogers, R. D. *Chem. Mater.* **1999**, *11*, 736. (r) Lu, J. Y.; Lawandy, M. A.; Li, J.; Yuan T.; Lin, C. L. *Inorg. Chem.* **1999**, *38*, 2695. (s) Lawandy, M. A.; Huang, X. Y.; Wang, R. J.; Li, J.; Lu, J. Y.; Yuen, T.; Lin, C. L. *Inorg. Chem.* **1999**, *38*, 5410. (t) Kou, H. Z.; Bu, W. M.; Liao, D. Z.; Jiang, Z. H.; Yan, S. P.; Fan, Y. G.; Wang G. L. *J. Chem. Soc., Dalton Trans.* **1998**, 4161.
- (2) Seo, J. S.; Whang, D.; Lee, H.; Jun, S. I.; Oh, J.; Jeon, Y. J.; Kim, K. *Nature* **2000**, *404*, 982.

Scheme 1



(H_a, H_b, H_c). Although H_a and H_b are both attached to carboxylic oxygen atoms, H_a can be deprotonated more easily, allowing the oxygen initially attached to it to form a chelating bond to a metal center with the adjacent nitrogen. The H_c in this ligand is linked to the nitrogen of the pyrazole ring and is more difficult to deprotonate than the two carboxylate hydrogen atoms. The multifunctional coordination sites of H₃pdcc and its ability to deprotonate at different acidity levels can, therefore, help us to invest the pH effect on the formation of coordination networks. Although a variety of coordination polymers containing transition metal elements have been synthesized, very few involve alkaline-earth metal centers.⁷ Herein we report a series of new coordination systems containing alkaline-earth metals and discuss the correlation between the reaction pH and structure dimensionality.

Experimental Section

Materials and Instruments. CaCl₂, SrCl₂·6H₂O, Sr(ClO₄)₂·6H₂O, BaCl₂, Ca(OH)₂, Sr(OH)₂·8H₂O, and Ba(OH)₂·8H₂O were purchased from Fisher and Alfa Aesar. 3,5-Pyrazoledicarboxylic acid monohydrate (97%) was purchased from Acros and triethylamine (99%+) from Alfa Aesar. All chemicals were used as received without further purification. Thermogravimetric analyses (TGA) were performed on a computer controlled TA Instrument TGA 2050 system under nitrogen flow and a scan rate of 5 °C/min. Infrared spectra were measured from a photoacoustics Model 300 on a Bio-Rad FTS-6000 IR system. Adsorption is described as usual: very strong (vs), strong (s), medium (m), shoulder (sh), weak (w), and broad (br). Powder X-ray diffraction (PXRD) of samples was performed on a Rigaku D/M-2200T automated diffraction system (Ultima⁺) at the operating power of 40kV/40mA, for polycrystalline samples of all compounds. The data were recorded at room temperature with a step size of 0.02 in 2θ and a scan speed of 1.7°/min. The analysis was carried out using the JADE (Windows) software package. The calculated PXRD patterns were generated from the single-crystal data.

[Ca(Hpdcc)(H₂O)₄]·2H₂O (1). Reaction of CaCl₂ (0.022 g, 0.2 mmol), H₃pdcc·H₂O (0.017 g, 0.1 mmol), and deionized water (10 mL, 0.5555 mol) in the mole ratio of 2:1:5555 (solution pH = 2.5) in a Teflon-lined bomb at 150 °C for 3 days yielded colorless solutions. After evaporation for several days at room temperature, colorless polyhedral crystals grew out of solution and were collected after filtration and drying (yield: 0.02 g, 67.8%). The final pH value remained the same (2.5). IR (4000–400 cm⁻¹): 3219(br), 1683.8(m),

1651.9(vs), 1559.6(m), 1506.5(m), 1459.1(s), 1436.8(m), 1393.3(m), 1209.1(s), 1111.0(m), 1018.8(sh), 818.3(m), 700.1(w).

[Ca(Hpdcc)(H₂O)₄]·H₂O (2). Reaction of CaCl₂ (0.0022 g, 0.2 mmol), H₃pdcc·H₂O (0.017 g, 0.1 mmol), Et₃N (0.028 mL, 0.2 mmol), and deionized water (10 mL, 0.5555 mol) in the mole ratio of 2:1:2:5555 (solution pH = 5) in a Teflon-lined bomb at 150 °C for 3 days produced a colorless solution. After evaporation for several days at room temperature, colorless platelike crystals of **2** were obtained via filtration and drying (yield: 0.021 g, 75.5%). The final pH value was 2.5. IR (400–4000 cm⁻¹): 3149.7(br), 2385.9(m), 1636.6(m), 1594.8-(sh), 1559.1(vs), 1519.7(s), 1454.2(s), 1371.2(vs), 1208.4(s), 1109.4-(m), 1007.9(s), 854.4(vs), 790.7(s), 718.7(w), 572.8(m).

[Ca(Hpdcc)(H₂O)] (3). Reaction of CaCl₂ (0.0022 g, 0.2 mmol), H₃pdcc·H₂O (0.017 g, 0.1 mmol), Et₃N (0.056 mL, 0.4 mmol), and deionized water (10 mL, 0.5555 mol) in the mole ratio of 2:1:4:5555 (solution pH = 9) in a Teflon-lined bomb at 150 °C for 3 days produced colorless columnlike crystals of **3** in high yield (0.0178 g, 86.0%). The final pH value was 6.0. This can also be synthesized by reacting of Ca(OH)₂ (0.037 g, 0.5 mmol), H₃pdcc·H₂O (0.085 g, 0.5 mmol), and deionized water (10 mL, 0.5555 mol) in the mole ratio of 1:1:1111 with pH at 11.5 at the same temperature and time period. The final pH value was 5. Colorless prism crystals were collected in quantitative yield (0.099 g, 93.5%). IR(4000–400 cm⁻¹): 3541.8(m), 3348.3(m), 3180.0(m), 3107.8(m), 2994.0(m), 2897.9(m), 2830.8(m), 2720.3(s), 2653.8(m), 2536.7(m), 2471.6(m), 2388.2(m), 2247.6(s), 1663.8(sh), 1581.7(s), 1564.0(s), 1516.4(vs), 1456.2(s), 1379.4(s), 1271.7(s), 1203.1(s), 1110.1(m), 1026.7(s), 1022.6(sh), 859.6(sh), 801.0(s), 744.7-(m), 656.6(m), 605.3(m).

[Sr(H₃pdcc)(H₂pdcc)₂(H₂O)₃]·2(H₃pdcc)·4H₂O (4). Reaction of Sr(ClO₄)₂ (0.04 g, 0.1 mmol), H₃pdcc·H₂O (0.017 g, 0.1 mmol), and deionized water (5 mL, 0.2778mol) in the mole ratio of 1:1:2778 (solution pH = 3) in a Teflon-lined bomb at 150 °C for 3 days yielded a colorless solution. The final pH value was 2.5. After evaporation for several days at room temperature, colorless prismatic crystals of **4** were isolated, along with an unknown powder.

[Sr(Hpdcc)(H₂O)] (5). Reaction of SrCl₂·6H₂O (0.0054 g, 0.2 mmol), H₃pdcc·H₂O (0.017 g, 0.1 mmol), Et₃N (0.028 mL, 0.2 mmol), and deionized water (5 mL, 0.2777 mol) in the mole ratio of 2:1:2:2778 (solution pH = 9) in a Teflon-lined bomb at 150 °C for 3 days produced colorless columnlike crystals of **5** in 61.0% yield (0.0155 g). The final pH value was 4. The compound can also be synthesized by reaction of Sr(OH)₂·8H₂O (0.013 g, 0.5 mmol), H₃pdcc·H₂O (0.085 g, 0.5 mmol), and deionized water (10 mL, 0.5555 mol) in the mole ratio of 1:1:1111 with pH at 3.0 under the same hydrothermal condition. The final pH value was 5. The colorless prism crystals were collected in high yield (0.1168 g, 91.9%). IR (400–4000 cm⁻¹): 3396.0(m), 3202.8-(m), 3107.8(w), 2994(m), 2886.9(m), 2817.9(m), 2706.1(m), 2626.3-(m), 2520.6(m), 1624.6(sh), 1599.6(s), 1558.9(vs), 1499.8(vs), 1455.9-(m), 1420.8(m), 1362.8(s), 1263.7(s), 1187.6(s), 1092.2(m), 1019.9(s), 1004.9(sh), 860.9(m), 830.7(sh), 795.9(s), 732.4(m), 658.7(s), 604.7-(w), 511.3(m).

[Ba(H₂pdcc)₂(H₂O)₄]·2H₂O (6). Reaction of BaCl₂ (0.0416 g, 0.2 mmol), H₃pdcc·H₂O (0.034 g, 0.2 mmol), and deionized water (5 mL, 0.2778mol) in the mole ratio of 1:1:1389 (solution pH = 3) in a Teflon-lined bomb at 150 °C for 3 days produced a colorless solution. Colorless, prismatic crystals of **6** were observed after the solution was evaporated for several days at room temperature. They were collected in 62.9% yield (0.017 g) following a filtration and drying procedure. The final pH value was 2.5. IR(4000–400 cm⁻¹): 3586.4(m), 3332–3217(br), 1700.4(s), 1648.8(vs), 1557.9(vs), 1501.6(s), 1454.3(m), 1318.6(w), 1194.7(m), 996.2(m), 858.2(m), 819.2(s), 777.1(s), 583.0-(s), 425.8(m).

[Ba(Hpdcc)(H₂O)] (7). Reaction of BaCl₂ (0.0416 g, 0.2 mmol), H₃pdcc·H₂O (0.017 g, 0.1 mmol), Et₃N (0.028 mL, 0.2 mmol), and deionized water (5 mL, 0.2777 mol) in the mole ratio of 2:1:2:2778 (solution pH = 9) in a Teflon-lined bomb at 150 °C for 3 days produced colorless platelike crystals of **7** in 72% yield (0.0435 g). The final pH value was 5. The compound can also be synthesized by reaction of Br(OH)₂·8H₂O (0.016 g, 0.5 mmol), H₃pdcc·H₂O (0.085 g, 0.5 mmol), and deionized water (10 mL, 0.5555 mol) in the mole ratio of 1:1:1111 with pH at 3.5 under the same hydrothermal conditions. The final

- (3) Mautner, F. A.; Cortés, R. Lezama, L.; Rojo, R. *Angew. Chem., Int. Ed. Engl.* **1996**, *35*, 78.
 (4) Noro, S.; Kitagawa, S.; Kondo, M.; Seki, K. *Angew. Chem., Int. Ed.* **2000**, *39*, 2082. (b) Chui, S. S.-Y.; Lo, S. M.-F.; Charmant, J. P. H.; Orpen, A. G.; Williams, I. D. *Science* **1999**, *283*, 1148. (c) Li, H.; Eddaoudi, M.; O'Keeffe, M.; Yaghi, O. M. *Science* **1999**, *402*, 276.
 (5) Li, H.; Eddaoudi, M.; Richardson, D. A.; Yaghi, O. M. *J. Am. Chem. Soc.* **1998**, *120*, 8567. (b) Li, H.; Laine, A.; O'Keeffe, M.; Yaghi, O. M. *Science* **1999**, *283*, 1145.
 (6) Gutschke, S. O. H.; Molinier, M.; Powell, A. K.; Winpenny, R. E. P.; Wood, P. T. *Chem. Commun.* **1996**, 823. (b) Pan, L.; Huang, X.; Li, J.; Wu, Y.; Zheng, N. *Angew. Chem., Int. Ed.* **2000**, *39*, 527. (c) Pan, L.; Huang, X.; Li, J. *J. Solid State Chem.* **2000**, *152*, 236.
 (7) Acharya, S. N. G.; Gopalan, R. S.; Kulkarni, G. U.; Venkatesan, K.; Bhattacharya, S. *Chem. Commun.* **2000**, 1351. (b) Platers, M. J.; Howie, R. A.; Orberts, A. *J. Chem. Commun.* **1997**, 893.

Table 1. Crystallographic Data for **1**, **2**, **3**, **4**, **5**, **6**, and **7**

	1	2	3	4	5	6	7
empirical formula	C ₅ H ₁₄ CaN ₂ O ₁₀	C ₅ H ₁₂ CaN ₂ O ₉	C ₅ H ₄ CaN ₂ O ₅	C ₄₀ H ₄₈ N ₁₆ O ₄₂ Sr ₂	C ₅ H ₄ N ₂ O ₅ Sr	C ₁₀ H ₁₈ Ba ₄ N ₄ O ₁₄	C ₁₀ H ₈ Ba ₂ N ₄ O ₁₀
fw	302.26	284.25	212.18	1600.18	259.72	555.62	618.88
space group	<i>P</i> ₂ ₁ / <i>n</i> (No.14)	<i>P</i> ₂ ₁ / <i>c</i> (No.14)	<i>P</i> ₂ ₁ / <i>c</i> (No.14)	<i>P</i> $\bar{1}$ (No.2)	<i>P</i> ₂ ₁ / <i>c</i> (No.14)	<i>C</i> ₂ / <i>c</i> (No.15)	<i>P</i> $\bar{1}$ (No.2)
<i>a</i> (Å)	8.382(2)	7.711(2)	6.616(1)	11.263(2)	9.213(2)	7.107(1)	7.107(1)
<i>b</i> (Å)	12.621(3)	15.574(3)	12.654(3)	11.460(3)	12.088(3)	6.708(1)	9.780(2)
<i>c</i> (Å)	11.767(2)	9.341(2)	8.782(2)	12.904(2)	6.196(2)	15.939(3)	11.431(2)
α	90	90	90	71.54(3)	90	90	74.69(3)
β (deg)	98.91(3)	96.73(3)	103.65(3)	98.96(3)	98.96(3)	123.56(3)	73.39(3)
γ	90	90	90	89.03(3)	90	90	85.29(3)
<i>V</i> (Å ³)	1229.8(5)	1114.0(4)	714.5(3)	1455.6(5)	681.6(2)	1825.8(6)	734.3(2)
<i>Z</i>	4	4	4	1	4	4	2
<i>T</i> (K)	293(2)	293(2)	293(2)	293(2)	293(2)	293(2)	293(2)
λ (Å)	0.71073	0.71073	0.71073	0.71073	0.71073	0.71073	0.71073
ρ_{calc} (g cm ⁻³)	1.633	1.695	1.973	1.825	2.531	2.021	2.799
μ (mm ⁻¹)	0.560	0.606	0.869	1.963	7.900	2.259	5.399
<i>R</i> ^a (<i>I</i> > 2 σ (<i>I</i>))	0.0397	0.0631	0.0575	0.0407	0.0373	0.0559	0.0422
<i>R</i> _w ^b	0.0759	0.1355	0.1030	0.0803	0.0809	0.0819	0.0883

^a $R = \sum ||F_o| - |F_c|| / \sum |F_o|$. ^b $R_w = [\sum [w(|F_o|^2 - |F_c|^2)|^2] / \sum w(F_o^2)^2]^{1/2}$. Weighting: **1**, $w = 1/\sigma^2[F_o^2 + (0.03 P)^2]$, where $P = (F_o^2 + 2F_c^2)/3$; **2**, $w = 1/\sigma^2(F_o^2 + 7.0 P)$; **3**, $w = 1/\sigma^2(F_o^2 + 4.0 P)$; **4**, $w = 1/\sigma^2[F_o^2 + (0.01 P)^2 + 2.0P]$; **5**, $w = 1/\sigma^2[F_o^2 + (0.04P)^2]$; **6**, $w = 1/\sigma^2(F_o^2)$; **7**, $1/\sigma^2[F_o^2 + (0.03P)^2]$.

Table 2. Selected Bond Lengths (Å) and Angles (deg) for **1**, **2**, and **3**^a

	1	2	3		
Ca—O(3) ⁱ	2.295(2)	Ca—O(1)	2.376(3)	Ca—O(3) ⁱ	2.347(5)
Ca—O(7)	2.348(2)	Ca—O(2) ⁱ	2.403(4)	Ca—O(5)	2.364(4)
Ca—O(5)	2.388(2)	Ca—O(5)	2.421(4)	Ca—O(4) ⁱⁱ	2.365(5)
Ca—O(1)	2.401(2)	Ca—O(7)	2.444(4)	Ca—O(2) ⁱⁱⁱ	2.386(4)
Ca—O(6)	2.446(2)	Ca—O(8)	2.458(4)	Ca—O(1)	2.433(4)
Ca—O(8)	2.454(2)	Ca—O(6)	2.464(4)	Ca—N(1)	2.514(5)
Ca—N(1)	2.565(2)	Ca—O(1) ⁱ	2.604(3)	Ca—O(1) ⁱⁱⁱ	2.536(4)
Ca—Ca ⁱ	6.867(2)	Ca—N(1)	2.655(4)	Ca—Ca ^{iv}	4.804(1)
		Ca—Ca ⁱ	4.754(1)	Ca—Ca ^v	7.256(2)
				Ca—Ca ^{vi}	6.616(1)
O(3) ⁱ —Ca—O(7)	82.12(8)	O(1)—Ca—O(2) ⁱ	150.49(12)	O(3) ⁱ —Ca—O(5)	89.20(17)
O(3) ⁱ —Ca—O(5)	89.69(7)	O(1)—Ca—O(5)	72.79(12)	O(3) ⁱ —Ca—O(4) ⁱⁱ	173.84(13)
O(7)—Ca—O(5)	155.33(8)	O(2) ⁱ —Ca—O(5)	80.14(13)	O(5)—Ca—O(4) ⁱⁱ	94.13(17)
O(3) ⁱ —Ca—O(1)	169.42(7)	O(1)—Ca—O(7)	94.24(13)	O(3) ⁱ —Ca—O(2) ⁱⁱⁱ	86.63(15)
O(7)—Ca—O(1)	101.25(7)	O(2) ⁱ —Ca—O(7)	92.72(14)	O(5)—Ca—O(2) ⁱⁱⁱ	131.22(15)
O(5)—Ca—O(1)	83.15(7)	O(5)—Ca—O(7)	80.59(14)	O(4) ⁱⁱ —Ca—O(2) ⁱⁱⁱ	87.28(15)
O(3) ⁱ —Ca—O(6)	82.57(7)	O(1)—Ca—O(8)	74.88(12)	O(3) ⁱ —Ca—O(1)	93.10(16)
O(7)—Ca—O(6)	78.46(8)	O(2) ⁱ —Ca—O(8)	87.00(13)	O(5)—Ca—O(1)	148.99(13)
O(5)—Ca—O(6)	77.43(8)	O(5)—Ca—O(8)	74.77(14)	O(4) ⁱⁱ —Ca—O(1)	86.72(15)
O(1)—Ca—O(6)	88.26(7)	O(7)—Ca—O(8)	155.04(13)	O(2) ⁱⁱⁱ —Ca—O(1)	79.79(13)
O(3) ⁱ —Ca—O(8)	79.00(7)	O(1)—Ca—O(6)	109.43(12)	O(3) ⁱ —Ca—N(1)	94.11(16)
O(7)—Ca—O(8)	119.83(8)	O(2) ⁱ —Ca—O(6)	87.78(13)	O(5)—Ca—N(1)	82.12(15)
O(5)—Ca—O(8)	80.88(8)	O(5)—Ca—O(6)	148.68(14)	O(4) ⁱⁱ —Ca—N(1)	91.48(16)
O(1)—Ca—O(8)	107.37(7)	O(7)—Ca—O(6)	129.12(13)	O(2) ⁱⁱⁱ —Ca—N(1)	146.65(15)
O(6)—Ca—O(8)	151.48(7)	O(8)—Ca—O(6)	75.83(12)	O(1)—Ca—N(1)	66.87(13)
O(3) ⁱ —Ca—N(1)	125.16(7)	O(1)—Ca—O(1) ⁱ	156.41(7)	O(3) ⁱ —Ca—O(1) ⁱⁱⁱ	87.15(15)
O(7)—Ca—N(1)	74.67(8)	O(2) ⁱ —Ca—O(1) ⁱ	51.87(11)	O(5)—Ca—O(1) ⁱⁱⁱ	78.26(13)
O(5)—Ca—N(1)	127.93(8)	O(5)—Ca—O(1) ⁱ	121.68(12)	O(4) ⁱⁱ —Ca—O(1) ⁱⁱⁱ	88.45(15)
O(1)—Ca—N(1)	65.37(7)	O(7)—Ca—O(1) ⁱ	72.02(12)	O(2) ⁱⁱⁱ —Ca—O(1) ⁱⁱⁱ	53.02(13)
O(6)—Ca—N(1)	137.06(8)	O(8)—Ca—O(1) ⁱ	125.00(12)	O(1)—Ca—O(1) ⁱⁱⁱ	132.73(6)
O(8)—Ca—N(1)	71.37(7)	O(6)—Ca—O(1) ⁱ	68.79(12)	N(1)—Ca—O(1) ⁱⁱⁱ	160.32(14)
		O(1)—Ca—N(1)	64.45(12)	C(1)—O(1)—Ca	120.8(3)
		O(2) ⁱ —Ca—N(1)	144.91(13)	C(1)—O(1)—Ca ^{iv}	88.7(3)
		O(5)—Ca—N(1)	128.72(14)	Ca—O(1)—Ca ^{iv}	150.43(16)
		O(7)—Ca—N(1)	75.87(13)		
		O(8)—Ca—N(1)	117.09(13)		
		O(6)—Ca—N(1)	75.21(13)		
		O(1) ⁱ —Ca—N(1)	93.12(11)		

^a Symmetry code for **1**: *i* = *x* - 1/2, -*y* + 3/2, *z* - 1/2. For **2**: *i* = *x*, -*y* + 1/2, *z* + 1/2. For **3**: *i* = -*x* + 1, *y* + 1/2, -*z* + 1/2; *ii* = -*x*, *y* + 1/2, -*z* + 1/2; *iii* = *x*, -*y* + 3/2, *z* - 1/2; *iv* = *x*, -*y* + 3/2, *z* + 1/2; *v* = -*x* + 1, *y* - 1/2, -*z* + 1/2; *vi* = *x* + 1, *y*, *z*.

pH value was 5. The colorless column crystals were collected in 82.2% yield (0.128 g). IR(400–4000 cm⁻¹): 3573.3(m), 3175(br), 3105.5(w), 2989.0(m), 2883.8(m), 2281.8(m), 2710.0(m), 2619.2(m), 1645.8(sh), 1615.4(sh), 1558.9(vs), 1506.7(vs), 1485.7(s), 1456.2(m), 1422.9(m), 1361.4(s), 1324.6(s), 1259.9(m), 1171.2(m), 1098.9(m), 1021.4(s), 997.4(s), 853.3(m), 825.5(w), 710.4(w), 516.5(m).

Crystal Structure Determination. Single-crystal structure analyses for compounds **1–7** were performed on an automated Enraf-Nonius CAD4. Single crystals with dimensions of 0.10 mm × 0.08 mm × 0.08 mm (**1**), 0.30 mm × 0.25 mm × 0.10 mm (**2**), 0.35 mm × 0.10 mm × 0.10 mm (**3**), 0.25 mm × 0.11 mm × 0.10 mm (**4**), 0.18 mm × 0.06 mm × 0.05 mm (**5**), 0.18 mm × 0.06 mm × 0.015 mm (**6**),

Table 3. Selected Bond Lengths (Å) and Angles (deg) for **4** and **5**^a

4							
Sr–O(1)	2.533(3)	Sr–O(18)	2.600(3)	Sr–O(19)	2.587(3)	Sr–O(9)	2.643(3)
Sr–O(5)	2.564(3)	Sr–O(3) ⁱ	2.638(3)	Sr–O(17)	2.592(3)	Sr–N(5)	2.682(3)
Sr–Sr ⁱ	9.694(5)						
O(1)–Sr–O(5)	144.78(9)	O(1)–Sr–O(3) ⁱ	92.37(10)	O(18)–Sr–O(9)		75.42(10)	
O(1)–Sr–O(19)	71.18(9)	O(5)–Sr–O(3) ⁱ	98.86(10)	O(3) ^j –Sr–O(9)		76.48(9)	
O(5)–Sr–O(19)	81.85(9)	O(19)–Sr–O(3) ⁱ	147.25(8)	O(1)–Sr–N(5)		81.70(9)	
O(1)–Sr–O(17)	78.13(10)	O(17)–Sr–O(3) ⁱ	71.23(9)	O(5)–Sr–N(5)		133.51(9)	
O(5)–Sr–O(17)	74.22(10)	O(18)–Sr–O(3) ⁱ	142.03(9)	O(19)–Sr–N(5)		130.48(9)	
O(19)–Sr–O(17)	77.63(9)	O(1)–Sr–O(9)	142.90(8)	O(17)–Sr–N(5)		136.47(10)	
O(1)–Sr–O(18)	94.86(12)	O(5)–Sr–O(9)	72.32(9)	O(18)–Sr–N(5)		72.73(11)	
O(5)–Sr–O(18)	96.42(12)	O(19)–Sr–O(9)	133.18(9)	O(3) ^j –Sr–N(5)		71.54(9)	
O(19)–Sr–O(18)	69.45(9)	O(17)–Sr–O(9)	128.43(9)	O(9)–Sr–N(5)		61.19(9)	
O(17)–Sr–O(18)	146.80(10)						
5							
Sr–O(4) ⁱ	2.528(3)	Sr–O(1)	2.633(3)	Sr–O(2)	2.714(4)	Sr–Sr ⁱⁱ	4.0767(10)
Sr–O(2) ⁱⁱ	2.570(4)	Sr–O(5) ^{iv}	2.694(4)	Sr–O(5)	2.736(4)	Sr–Sr ^{viii}	4.4016(8)
Sr–O(3) ⁱⁱⁱ	2.597(4)	Sr–O(3) ^v	2.705(4)	Sr–O(4) ^{vi}	2.796(3)	Sr–Sr ^x	4.448(1)
O(4) ⁱ –Sr–O(2) ⁱⁱ	137.03(12)	O(5) ^{iv} –Sr–O(3) ^v	68.19(11)	O(2)–Sr–O(5)		136.45(11)	
O(4) ⁱ –Sr–O(3) ⁱⁱⁱ	142.23(12)	O(4) ⁱ –Sr–O(2)	123.36(11)	O(4) ⁱ –Sr–O(4) ^{vi}		77.00(8)	
O(2) ⁱⁱ –Sr–O(3) ⁱⁱⁱ	75.81(11)	O(2) ⁱⁱ –Sr–O(2)	79.05(12)	O(2) ⁱⁱ –Sr–O(4) ^{vi}		73.46(11)	
O(4) ⁱ –Sr–O(1)	74.75(11)	O(3) ⁱⁱⁱ –Sr–O(2)	72.48(11)	O(3) ⁱⁱⁱ –Sr–O(4) ^{vi}		139.90(11)	
O(2) ⁱⁱ –Sr–O(1)	119.11(11)	O(1)–Sr–O(2)	48.81(10)	O(1)–Sr–O(4) ^{vi}		66.80(11)	
O(3) ⁱⁱⁱ –Sr–O(1)	108.39(11)	O(5) ^{iv} –Sr–O(2)	147.20(11)	O(5) ^{iv} –Sr–O(4) ^{vi}		135.62(11)	
O(4) ⁱ –Sr–O(5) ^{iv}	71.54(11)	O(3) ^v –Sr–O(2)	84.66(11)	O(3) ^v –Sr–O(4) ^{vi}		136.00(10)	
O(2) ⁱⁱ –Sr–O(5) ^{iv}	110.69(11)	O(4) ⁱ –Sr–O(5)	71.93(11)	O(2)–Sr–O(4) ^{vi}		76.89(10)	
O(3) ⁱⁱⁱ –Sr–O(5) ^{iv}	79.59(11)	O(2) ⁱⁱ –Sr–O(5)	68.14(11)	O(5)–Sr–O(4) ^{vi}		67.05(10)	
O(1)–Sr–O(5) ^{iv}	130.07(11)	O(3) ⁱⁱⁱ –Sr–O(5)	122.79(11)	Sr ⁱⁱ –O(2)–Sr		100.95(12)	
O(4) ⁱ –Sr–O(3) ^v	80.75(11)	O(1)–Sr–O(5)	127.57(11)	Sr ^{viii} –O(3)–Sr ^v		114.05(13)	
O(2) ⁱⁱ –Sr–O(3) ^v	141.41(11)	O(5) ^{iv} –Sr–O(5)	73.84(7)	Sr ^{ix} –O(4)–Sr ^{vi}		111.43(12)	
O(3) ⁱⁱⁱ –Sr–O(3) ^v	65.95(13)	O(3) ^v –Sr–O(5)	138.57(11)	Sr ^{vii} –O(5)–Sr		108.31(12)	
O(1)–Sr–O(3) ^v	70.94(11)						

^a Symmetry code for **4**: i = -x + 1, -y + 1, -y + 2. For **5**: i = -x + 1, y - 1/2, -y + 1/2; ii = -x, -y + 1, -y; iii = x - 1, y, y; iv = x, -y + 1/2, y + 1/2; v = -x + 1, -y + 1, -y + 1; vi = -x + 1, -y + 1, -y; vii = x, -y + 1/2, y - 1/2; viii = x + 1, y, y; ix = -x + 1, y + 1/2, -y + 1/2; x = -x, -y + 1, -y + 1.

Table 4. Selected Bond Lengths (Å) and Angles (deg) for **6**^a

Ba–O(5)	2.792(6)	Ba–O(3) ⁱⁱⁱ	2.798(5)	Ba–O(6) ⁱ	2.934(6)	Ba–N(1) ^j	3.000(5)
Ba–O(5) ⁱ	2.792(6)	Ba–O(1)	2.851(4)	Ba–O(6)	2.934(6)	Ba–Ba ⁱⁱⁱ	8.856(4)
Ba–O(3) ⁱⁱ	2.798(5)	Ba–O(1) ⁱ	2.851(4)	Ba–N(1)	3.000(5)		
O(5)–Ba–O(5) ⁱ	63.4(2)	O(5)–Ba–O(6) ⁱ	133.89(15)	O(3) ⁱⁱⁱ –Ba–N(1)		118.55(15)	
O(5)–Ba–O(3) ⁱⁱ	137.29(17)	O(5) ⁱ –Ba–O(6) ⁱ	132.96(16)	O(3) ⁱⁱⁱ –Ba–N(1)		69.76(15)	
O(5) ⁱ –Ba–O(3) ⁱⁱ	76.55(17)	O(3) ⁱⁱⁱ –Ba–O(6) ⁱ	66.49(16)	O(1)–Ba–N(1)		55.60(14)	
O(5)–Ba–O(3) ⁱⁱⁱ	76.55(17)	O(3) ⁱⁱⁱ –Ba–O(6) ⁱ	85.54(16)	O(1) ⁱ –Ba–N(1)		124.07(14)	
O(5) ⁱ –Ba–O(3) ⁱⁱⁱ	137.29(18)	O(1)–Ba–O(6) ⁱ	115.14(17)	O(6) ^j –Ba–N(1)		138.32(16)	
O(3) ⁱⁱ –Ba–O(3) ⁱⁱⁱ	145.7(3)	O(1) ⁱ –Ba–O(6) ⁱ	65.92(17)	O(6)–Ba–N(1)		67.31(16)	
O(5)–Ba–O(1)	110.84(17)	O(5)–Ba–O(6)	132.96(16)	O(5)–Ba–N(1) ^j		84.59(17)	
O(5) ⁱ –Ba–O(1)	68.07(18)	O(5) ⁱ –Ba–O(6)	133.89(15)	O(5) ⁱ –Ba–N(1) ^j		73.38(17)	
O(3) ⁱⁱ –Ba–O(1)	63.08(13)	O(3) ⁱⁱⁱ –Ba–O(6)	85.54(16)	O(3) ⁱⁱⁱ –Ba–N(1) ^j		69.76(15)	
O(3) ⁱⁱⁱ –Ba–O(1)	117.31(13)	O(3) ⁱⁱⁱ –Ba–O(6)	66.49(16)	O(3) ⁱⁱⁱ –Ba–N(1) ^j		118.55(15)	
O(5)–Ba–O(1) ⁱ	68.07(18)	O(1)–Ba–O(6)	65.92(17)	O(1)–Ba–N(1) ^j		124.07(14)	
O(5) ⁱ –Ba–O(1) ⁱ	110.84(17)	O(1) ⁱ –Ba–O(6)	115.14(17)	O(1) ⁱ –Ba–N(1) ^j		55.60(14)	
O(3) ⁱⁱ –Ba–O(1) ⁱ	117.31(13)	O(6) ^j –Ba–O(6)	72.2(2)	O(6) ^j –Ba–N(1) ^j		67.31(16)	
O(3) ⁱⁱⁱ –Ba–O(1) ⁱ	63.08(13)	O(5)–Ba–N(1)	73.38(17)	O(6)–Ba–N(1) ^j		138.32(16)	
O(1)–Ba–O(1) ⁱ	178.8(3)	O(5) ⁱ –Ba–N(1)	84.59(17)	N(1)–Ba–N(1) ^j		154.2(3)	

^a Symmetry code for **6**: i = -x + 1, y, -z + 3/2; ii = x + 1/2, -y + 3/2, z + 1/2; iii = -x + 1/2, -y + 3/2, -z + 1.

and 0.06 mm × 0.05 mm × 0.025 mm (**7**) were selected for the crystal structure analyses. Each crystal was mounted on a glass fiber and placed onto the goniometer head in air. Lattice parameters were obtained from least-squares analyses of 25 computer-centered reflections with 8.45° ≤ θ ≤ 13.91° (**1**), 7.85° ≤ θ ≤ 10.63° (**2**), 7.00° ≤ θ ≤ 12.78° (**3**), 7.99° ≤ θ ≤ 13.35° (**4**), 7.75° ≤ θ ≤ 13.87° (**5**), 9.22° ≤ θ ≤ 13.53° (**6**), and 6.90° ≤ θ ≤ 10.00° (**7**) using graphite-monochromated Mo Kα radiation (λ = 0.71073 Å). All data were collected at room temperature 293(2) K with ω-scan method within the limits 2° < θ < 26°. The data collections for all crystals were monitored by three standards every 4 h and raw intensities were corrected for Lorentz and

polarization effects and for absorption by empirical method based on ψ-scan data.⁸ No decay was observed. Direct methods yielded the positions of metals. The remaining non-hydrogen atoms were located from the subsequent difference Fourier synthesis. Hydrogen atoms were located from difference Fourier maps but were not refined and their thermal parameters were set equal to 1.2 × U_{eq} of the parent non-hydrogen atoms. All of the non-hydrogen atoms were subjected to anisotropic refinement. Data collections were controlled by the CAD4/PC program package. All calculations were performed using the

(8) Kopfmann, G.; Hubber R. *Acta Crystallogr.* **1968**, *A24*, 348.

Table 5. Selected Bond Lengths (Å) and Angles (deg) for **7**^a

Ba(1)–O(5)	2.723(6)	Ba(1)–N(3)	3.029(7)	Ba(2)–O(2) ^v	2.754(6)	Ba(2)–O(1)	2.854(5)
Ba(1)–O(4) ⁱ	2.741(5)	Ba(1)–O(8) ⁱⁱⁱ	3.029(7)	Ba(2)–O(7) ⁱⁱⁱ	2.777(6)	Ba(2)–O(10) ^{viii}	2.868(6)
Ba(1)–O(8) ⁱⁱⁱ	2.742(6)	Ba(1)–N(1)	3.162(8)	Ba(2)–O(10)	2.820(6)	Ba(2)–O(3) ⁱⁱⁱ	2.871(6)
Ba(1)–O(1)	2.766(6)	Ba(2)–O(6) ^{iv}	2.746(6)	Ba(2)–O(3) ^{vi}	2.831(6)	Ba(2)–O(5) ^{iv}	3.248(6)
Ba(1)–O(9)	2.787(6)	Ba(1)–Ba(2)	4.4243(12)	Ba(2)–O(9)	2.846(7)	Ba(2)–Ba(2) ^{vii}	4.0771(15)
Ba(1)–O(7) ⁱⁱⁱ	2.932(6)						
O(5)–Ba(1)–O(4) ⁱ	136.75(18)	O(8) ⁱⁱ –Ba(1)–N(1)	148.82(17)	O(7) ⁱⁱⁱ –Ba(2)–O(10) ^{vii}	123.29(17)		
O(5)–Ba(1)–O(8) ⁱⁱⁱ	75.3(2)	O(1)–Ba(1)–N(1)	55.21(18)	O(10)–Ba(2)–O(10) ^{vii}	88.43(16)		
O(4) ⁱ –Ba(1)–O(8) ⁱⁱⁱ	68.41(19)	O(9)–Ba(1)–N(1)	70.2(2)	O(3) ^{vi} –Ba(2)–O(10) ^{vii}	57.84(18)		
O(5)–Ba(1)–O(1)	150.61(17)	O(7) ⁱⁱⁱ –Ba(1)–N(1)	106.81(17)	O(9)–Ba(2)–O(10) ^{vii}	127.8(2)		
O(4) ⁱ –Ba(1)–O(1)	72.12(17)	N(3)–Ba(1)–N(1)	69.90(19)	O(1)–Ba(2)–O(10) ^{vii}	72.54(16)		
O(8) ⁱⁱⁱ –Ba(1)–O(1)	131.79(18)	O(8) ⁱⁱⁱ –Ba(1)–N(1)	145.81(16)	O(6) ^{iv} –Ba(2)–O(3) ⁱⁱⁱ	67.81(18)		
O(5)–Ba(1)–O(9)	78.72(19)	O(6) ^{iv} –Ba(2)–O(2) ^v	79.39(19)	O(2) ^v –Ba(2)–O(3) ⁱⁱⁱ	73.96(17)		
O(4) ⁱ –Ba(1)–O(9)	144.51(18)	O(6) ^{iv} –Ba(2)–O(7) ⁱⁱⁱ	89.77(19)	O(7) ⁱⁱⁱ –Ba(2)–O(3) ⁱⁱⁱ	135.76(18)		
O(8) ⁱⁱⁱ –Ba(1)–O(9)	139.2(2)	O(2) ^v –Ba(2)–O(7) ⁱⁱⁱ	64.41(17)	O(10)–Ba(2)–O(3) ⁱⁱⁱ	57.92(17)		
O(1)–Ba(1)–O(9)	72.46(18)	O(6) ^{iv} –Ba(2)–O(10)	68.5(2)	O(3) ^{vi} –Ba(2)–O(3) ⁱⁱⁱ	88.70(17)		
O(5)–Ba(1)–O(7) ⁱⁱⁱ	111.41(18)	O(2) ^v –Ba(2)–O(10)	129.09(18)	O(9)–Ba(2)–O(3) ⁱⁱⁱ	155.76(17)		
O(4) ⁱ –Ba(1)–O(7) ⁱⁱⁱ	97.20(17)	O(7) ⁱⁱⁱ –Ba(2)–O(10)	148.27(18)	O(1)–Ba(2)–O(3) ⁱⁱⁱ	129.25(16)		
O(8) ⁱⁱⁱ –Ba(1)–O(7) ⁱⁱⁱ	99.32(17)	O(6) ^{iv} –Ba(2)–O(3) ^{vi}	129.25(18)	O(10) ^{vii} –Ba(2)–O(3) ⁱⁱⁱ	59.93(16)		
O(1)–Ba(1)–O(7) ⁱⁱⁱ	59.37(17)	O(2) ^v –Ba(2)–O(3) ^{vi}	138.03(18)	O(6) ^{iv} –Ba(2)–O(5) ^{iv}	42.40(16)		
O(9)–Ba(1)–O(7) ⁱⁱⁱ	62.1(2)	O(7) ⁱⁱⁱ –Ba(2)–O(3) ^{vi}	132.61(16)	O(2) ^v –Ba(2)–O(5) ^{iv}	106.55(18)		
O(5)–Ba(1)–N(3)	57.63(19)	O(10)–Ba(2)–O(3) ^{vi}	60.95(17)	O(7) ⁱⁱⁱ –Ba(2)–O(5) ^{iv}	73.55(17)		
O(4) ⁱ –Ba(1)–N(3)	98.48(18)	O(6) ^{iv} –Ba(2)–O(9)	102.6(2)	O(10)–Ba(2)–O(5) ^{iv}	74.86(17)		
O(8) ⁱⁱⁱ –Ba(1)–N(3)	89.22(19)	O(2) ^v –Ba(2)–O(9)	127.69(19)	O(3) ^{vi} –Ba(2)–O(5) ^{iv}	115.01(17)		
O(1)–Ba(1)–N(3)	123.43(19)	O(7) ⁱⁱⁱ –Ba(2)–O(9)	63.34(19)	O(9)–Ba(2)–O(5) ^{iv}	60.30(19)		
O(9)–Ba(1)–N(3)	102.8(2)	O(10)–Ba(2)–O(9)	97.99(18)	O(1)–Ba(2)–O(5) ^{iv}	123.38(16)		
O(7) ⁱⁱⁱ –Ba(1)–N(3)	164.04(16)	O(3) ^{vi} –Ba(2)–O(9)	80.5(2)	O(10) ^{vii} –Ba(2)–O(5) ^{iv}	162.78(16)		
O(5)–Ba(1)–O(8) ⁱⁱⁱ	77.30(19)	O(6) ^{iv} –Ba(2)–O(1)	149.47(19)	O(3) ⁱⁱⁱ –Ba(2)–O(5) ^{iv}	106.31(16)		
O(4) ⁱ –Ba(1)–O(8) ⁱⁱⁱ	106.48(19)	O(2) ^v –Ba(2)–O(1)	82.22(17)	Ba(1)–O(1)–Ba(2)	103.86(18)		
O(8) ⁱⁱⁱ –Ba(1)–O(8) ⁱⁱⁱ	65.11(19)	O(7) ⁱⁱⁱ –Ba(2)–O(1)	60.21(17)	Ba(2) ^{vi} –O(3)–Ba(2) ^{viii}	91.30(17)		
O(1)–Ba(1)–O(8) ⁱⁱⁱ	102.20(17)	O(10)–Ba(2)–O(1)	140.78(19)	Ba(1)–O(5)–Ba(2) ^{iv}	148.6(2)		
O(9)–Ba(1)–O(8) ⁱⁱⁱ	78.9(2)	O(3) ^{vi} –Ba(2)–O(1)	79.99(17)	Ba(2) ^{viii} –O(7)–Ba(1) ^{viii}	101.55(19)		
O(7) ⁱⁱⁱ –Ba(1)–O(8) ⁱⁱⁱ	43.30(16)	O(9)–Ba(2)–O(1)	70.32(18)	Ba(1) ⁱⁱ –O(8)–Ba(1) ^{viii}	114.89(19)		
N(3)–Ba(1)–O(8) ⁱⁱⁱ	132.95(18)	O(6) ^{iv} –Ba(2)–O(10) ^{vii}	127.32(18)	Ba(1)–O(9)–Ba(2)	103.5(2)		
O(5)–Ba(1)–N(1)	109.4(2)	O(2) ^v –Ba(2)–O(10) ^{vii}	80.62(19)	Ba(2)–O(10)–Ba(2) ^{vii}	91.57(16)		
O(4) ⁱ –Ba(1)–N(1)	91.35(19)						

^a Symmetry code for **7**: i = $-x + 2, -y + 1, -z + 1$; ii = $-x + 2, -y + 1, -z + 2$; iii = $x, y - 1, z$; iv = $-x + 1, -y, -z + 2$; v = $-x + 2, -y, -z + 1$; vi = $-x + 1, -y + 1, -z + 1$; vii = $-x + 1, -y, -z + 1$; viii = $x, y + 1, z$.

SHELX97 software packages.⁹ Analytic expressions of atomic scattering factors were employed, and anomalous dispersion corrections were incorporated.¹⁰ The final full-matrix, least-squares refinement on F^2 was applied for all independent reflections ($I > 2\sigma(I)$) and variables. Crystal drawings were produced by SCHAKAL 97.¹¹ Details of data collection and structure refinement, along with unit cell parameters for **1**, **2**, **3**, **4**, **5**, **6**, and **7**, are listed in Table 1. Selected bond lengths and angles for all structures are given in Tables 2–5.

Results and Discussion

Structures. Hydrothermal method was employed in this work for the synthesis and crystal growth of the title compounds. This method has proven to be an effective and simple technique for crystal growth of inorganic materials under autogenous pressure.¹² One of its advantages over a number of others (e.g., diffusion and sol–gel techniques) is the effective use of inorganic and organic reagents with low solubility. Even insoluble precursors can be used in situ with this method.¹³

While the problem for accurate prediction of crystal architectures remains unsolved,¹⁴ our efforts throughout this work have been to understand the influence of certain reaction parameters, such as pH, on the crystal structures of the products. A trend, and consequently a correlation, between the reaction acidity and the dimensionality of the resultant structures should become apparent after a careful comparison.

The soluble complexes **1**, **2**, **4**, and **6** with lower dimensionality were synthesized from solutions with relatively low pH. Adjusting the reaction conditions by adding a basic solvent, such as Et₃N, or by including in the reaction a basic reagent, M(OH)₂, resulted in insoluble, three-dimensional complexes **3**, **5**, and **7**. Three different structures were obtained for the Ca(II) compounds. At lower pH levels the two one-dimensional structures **1** and **2** were formed. A higher pH solution produced the three-dimensional structure **3**. The structures of **1** and **2** consist of infinite zigzag chains built by tetra-aqua-calcium and bridging Hpd²⁻ groups. The coordination polyhedra around Ca(II) ions can be attributed to a capped trigonal prism in **1** (Figure 1a) and a trigonal dodecahedron in **2** (Figure 3a), respectively. In structure **1**, as shown in Figure 1b, the capped position is occupied by an O_{6w} atom from a coordinated water (where w stands for a water molecule). The trigonal prism is comprised of two Hpd²⁻ ligands, one coordinated to the metal center in chelating fashion (referred to a five-membered chelate ring) through the carboxylate oxygen (O1) as well as its adjacent

(9) Sheldrick, G. M. *SHELX-97: program for structure refinement*; University of Goettingen: Goettingen, Germany, 1997.

(10) *International Tables for X-ray Crystallography*; Kluwer Academic Publishers: Dordrecht, 1989; Vol. C, Tables 4.2.6.8 and 6.1.1.4.

(11) Keller, E. *SCHAKAL97: a computer program for graphical representation of Molecular and crystallographic models*; University of Freiburg: Freiburg, Germany, 1997.

(12) Laudise, R. A. In *Progress in Inorganic Chemistry*; Interscience Publishers: New York, 1962; Vol. 3. (b) Rabenau, A. *Angew. Chem., Int. Ed. Engl.* **1985**, *24*, 1026. (c) Haushalter, R. C.; Mundi, L. A. *Chem. Mater.* **1982**, *4*, 31 and references therein. (d) Hagrman, D.; Hagrman, P. J.; Zubieta, J. *Angew. Chem., Int. Ed.* **1999**, *38*, 3165.

(13) Koene, G. E.; Taylor, N. J.; Nazar, L. F.; *Angew. Chem., Int. Ed.* **1999**, *38*, 2888.

(14) Maddox, J. *Nature* **1988**, *335*, 201.

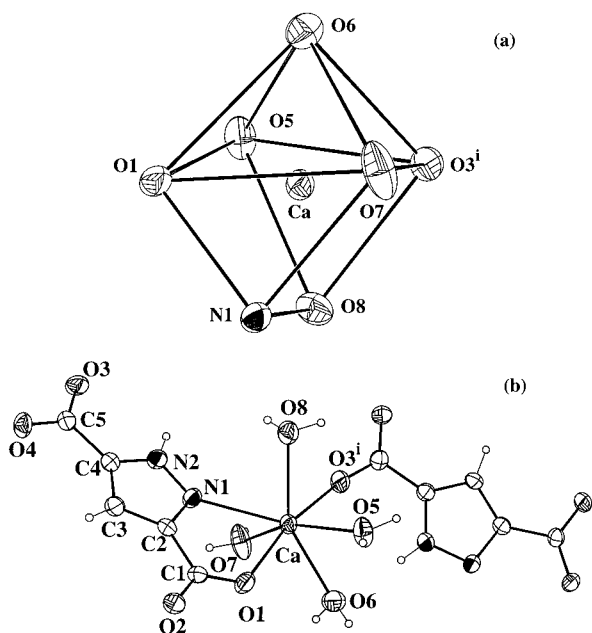


Figure 1. (a) Coordination polyhedron around the Ca metal in **1**. (b) Coordination environment of **1** (ORTEP drawing with 50% probability of ellipsoids).

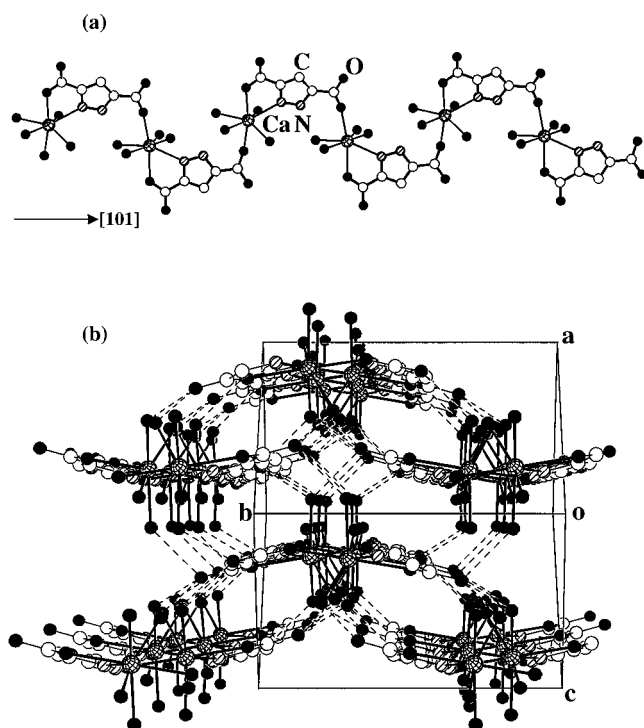


Figure 2. (a) View of the one-dimensional chain along [101] in **1**. The cross-shaded circles are Ca atoms, the solid circles are O atoms, the shaded circles are N atoms, and the open circles are C atoms. The H atoms are omitted for clarity. (b) View down the [101] axis showing packing of the chains and the three-dimensional hydrogen-bonding network in **1**. The H atoms and the lattice water are omitted for clarity.

nitrogen atom (N1) in the pyrazole ring, the other coordinated to the metal through the monodentate carboxylate group (O3ⁱ). The remaining three sites of the prism are occupied by oxygen atoms (O5w, O7w, O8w) from coordinated waters. The zigzag chain is formed by equally distanced Ca (Ca...Ca: 6.867(2) Å) connected via bridging Hpdc²⁻ and is parallel to the [101] direction (Figure 2a). The three oxygen atoms of the coordinated

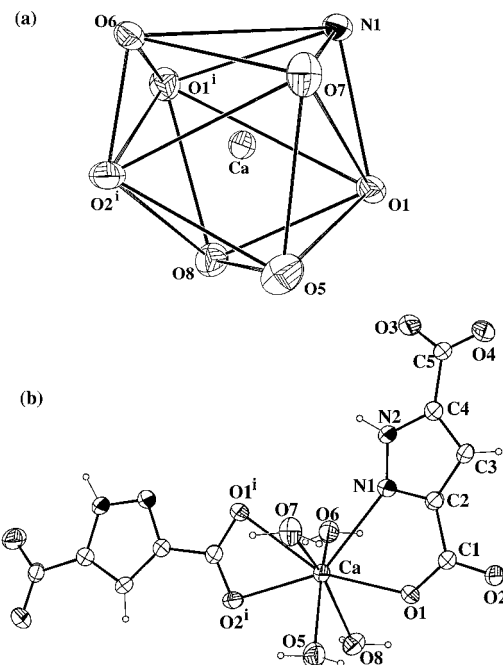


Figure 3. (a) Coordination polyhedron around Ca in **2**. (b) Coordination environment of **2** (ORTEP drawing with 50% probability of ellipsoids).

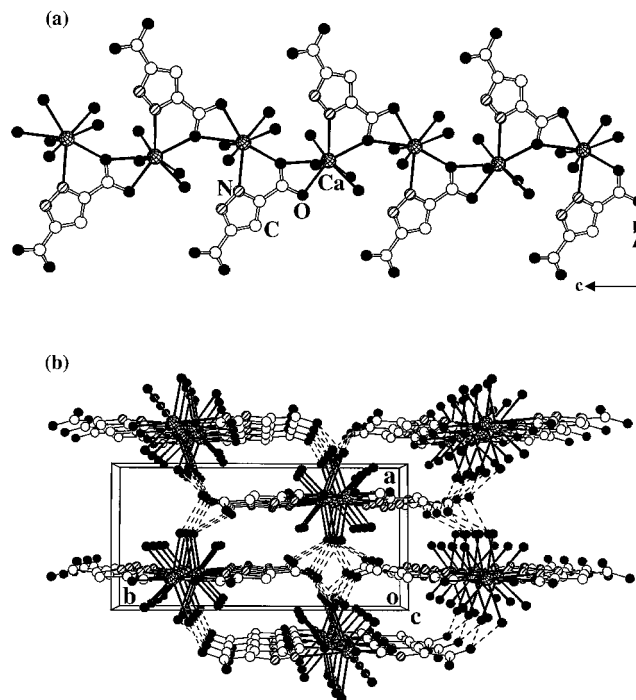


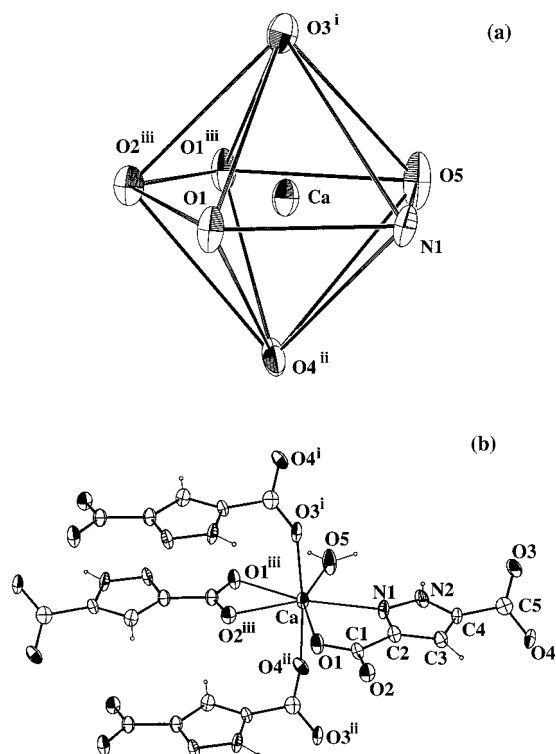
Figure 4. (a) View of the 1D chain along the *c*-axis in **2**. The same labeling scheme as that used in Figure 2 is used here. The H atoms are omitted for clarity. (b) View down the *c*-axis showing packing of the chains and H-bonding network in **2**. The H atoms and the lattice water are omitted for clarity.

water (O5w, O7w, O8w) in each chain are engaged in five hydrogen bonds, ranging from 2.761 to 2.822 Å, with the carboxyl oxygen atoms of four adjacent chains to yield a three-dimensional structure held by hydrogen-bonding (Figure 2b). The fourth coordinated water (O6w) forms an intrachain hydrogen bond with the pyrazole nitrogen (N2-H13...O6, 2.947(3) Å). Two lattice water molecules form a number of hydrogen bonds with carboxyl oxygen atoms, coordinated water,

Table 6. Selected Hydrogen Bond Distances (Å) for **1**, **2**, **4**, and **6**

D... A	symmetry code of A	distances	D... A	symmetry code of A	distances
1					
O(5)···O(2)	$(-x - 1/2, y - 1/2, -z + 1/2)$	2.818(3)	O(5)···O(7)	$(x, -y + 1/2, z - 1/2)$	2.948(5)
O(5)···O(4)	$(-x, -y + 2, -z + 1)$	2.819(3)	O(6)···O(3)	$(-x + 1, y - 1/2, -z + 1/2)$	2.738(5)
O(7)···O(4)	$(-x + 1, -y + 2, -z + 1)$	2.761(3)	O(6)···O(4)	$(-x + 1, -y + 1, -z)$	2.776(5)
O(7)···O(2)	$(-x + 1/2, y - 1/2, -z + 1/2)$	2.806(3)	O(7)···O(4)	$(-x + 2, -y + 1, -z)$	2.808(5)
O(8)···O(2)	$(-x, -y + 2, -z + 1)$	2.822(3)	O(7)···O(4)	$(-x + 2, y - 1/2, -z + 1/2)$	3.052(5)
N(2)···O(6)	$(x + 1/2, -y + 3/2, z + 1/2)$	2.947(3)	O(8)···O(6)	$(x, -y + 1/2, z - 1/2)$	2.849(5)
4					
O(2)···O(14)	$(-x + 2, -y + 2, -z + 2)$	2.716(4)	O(4)···O(1)	$(x - 1/2, -y + 3/2, z - 1/2)$	2.499(6)
O(6)···O(9)	(x, y, z)	2.816(4)	O(5)···O(6)	$(-x + 1, y - 1, -z + 3/2)$	3.015(8)
O(8)···O(13)	$(-x + 3, -y + 2, -z + 1)$	2.447(4)	O(5)···O(2)	$(x, -y + 1, z - 1/2)$	2.705(7)
O(10)···O(4)	$(x + 1, y, z - 1)$	2.488(4)	O(6)···O(5)	$(x, y + 1, z)$	2.982(8)
O(17)···N(7)	$(-x + 2, -y + 2, -z + 2)$	2.791(4)			
O(18)···O(7)	$(x - 1, y, z)$	2.847(4)			
O(18)···O(18)	$(-x + 2, -y + 2, -z + 1)$	3.012(4)			
O(19)···O(14)	$(-x + 2, -y + 2, -z + 2)$	2.813(4)			
O(19)···N(7)	$(-x + 2, -y + 2, -z + 2)$	3.099(4)			
O(19)···O(7)	$(-x + 3, -y + 2, -z + 1)$	2.775(4)			
N(2)···O(11)	(x, y, z)	2.859(4)			
N(4)···O(16)	$(-x + 2, -y + 2, -z + 2)$	2.839(4)			
N(6)···N(1)	(x, y, z)	2.821(4)			
N(8)···N(3)	$(-x + 2, -y + 2, -z + 2)$	2.852(4)			

and among themselves. Selected hydrogen bond distances are given in Table 6. In structure **2**, as illustrated in Figure 3, the coordination of the calcium metal can be described as a distorted trigonal dodecahedron which contains two Hpdc^{2-} ligands, one coordinating to the metal in a chelating fashion as in **1** (O1, N1) while the other using O2ⁱ and O1ⁱ to form a four-membered chelate ring with the metal. The remaining sites are occupied by oxygen atoms (O5w, O6w, O7w, O8w) from four coordinated water. The neighboring calcium atoms are equally spaced (4.754(1) Å) and bridged by a single Hpdc^{2-} via two types of aforementioned four- and five-membered chelating rings to form a zigzag chain along the *c*-axis (see Figure 4a). The η^2 -oxygen bonded to the two neighboring Ca gives Ca–O distances of 2.376(3) and 2.604(3) Å, respectively. Selected hydrogen bond distances for **2** are listed in Table 6. A three-dimensional hydrogen-bonded network is comprised of the coordinated water (O5w, O6w, O7w) with uncoordinated carboxyl oxygen atoms (O3, O4) of Hpdc^{2-} from the adjacent chains (Figure 4b). The hydrogen bonds resulting from pyrazole nitrogen and coordinated water N2–H11···O8 (2.925 Å), and among the coordinated water (O5–H1···O7, 2.948(5) Å, O8–H8···O6, 2.849(5) Å), also form intrachain interactions as in **1**. Yet, unlike in **1**, the lattice water (O9w) involved in hydrogen-bonding with carboxyl oxygen atoms (O2, O3) and oxygen atoms from the coordinated water (O5) do not form any hydrogen bonds among themselves. When the pH value was increased to 6, three-dimensional structure **3** resulted via covalent bond. The coordination polyhedron around Ca(II) in this structure can be attributed to a pentagonal bipyramid, as illustrated in Figure 5a. The pentagonal plane consists of two chelating Hpdc^{2-} , one via carboxyl oxygen atoms (O1ⁱⁱⁱ and O2ⁱⁱⁱ) and the other via carboxyl oxygen (O1) coming from another carboxylate group and its adjacent nitrogen atom (N1); the coordinated water lies on the fifth site via its O5. The apical sites are taken by two monodentate carboxylate ions, O3ⁱ and O4ⁱⁱ. As in **1**, **3** also has a η^2 -oxygen with Ca–O1 and Ca^{iv}–O1 distances of 2.433(4) and 2.536(4) Å, respectively. It is worth noting that **3** is isostructural to that of a cadmium compound obtained at low pH value.^{6c} The structure of **3** may be described as the following: each calcium atom is coordinated by N1, O1 of a Hpdc^{2-} to form a five-member chelating ring and O1ⁱⁱⁱ, O2ⁱⁱⁱ of

**Figure 5.** (a) Coordination polyhedron around Ca in **3**. (b) Coordination environment of **3** (ORTEP drawing with 50% probability of ellipsoids).

the second Hpdc^{2-} to form a four-membered chelate ring. A zigzag ribbon running parallel to the *c*-axis results by connecting neighboring metal centers with a single bridging Hpdc^{2-} , as shown in Figure 6a. The essential difference between **3** and **2**, in addition to the strikingly different metal coordination polyhedra, is the inter-ribbon connection. In **3**, they are connected through O3ⁱ and O4ⁱⁱ atoms (and O3ⁱⁱⁱ and O4ⁱⁱⁱ, see Figure 5b) which coordinate to one Ca above and another Ca below the plane of the chain in an *anti-anti* mode.¹⁵ This result

(15) Mehrotra, C.; Bohra, R. *Metal Carboxylates*; Academic Press: New York, 1983.

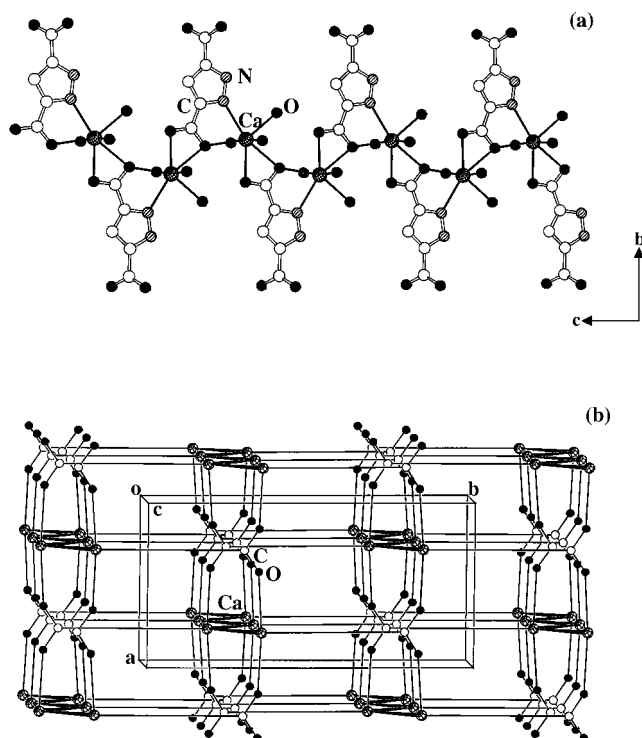


Figure 6. (a) View of the 1D chain along the *c*-axis in **3**. The same labeling scheme as that used in Figure 2 is used here. The H atoms are omitted for clarity. (b) The simplified three-dimensional structure of **3** showing interchain bonding patterns. Only the metals and carboxylate ions in *anti-anti* bonding mode are drawn.

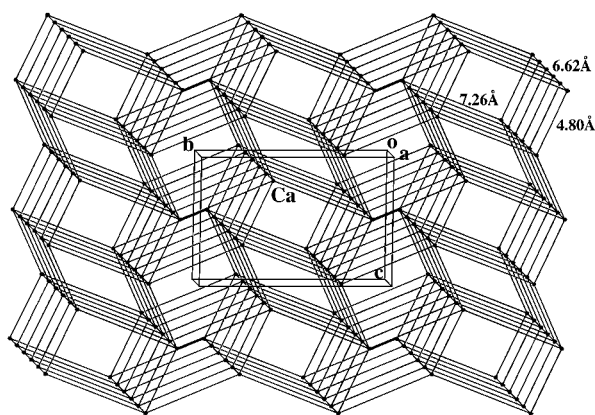


Figure 7. Schematic presentation showing the connectivity among the metal atoms in **3**.

in a three-dimensional structure plotted in Figure 6b. The nearest metal–metal distance in the zigzag chain is 4.804(1) Å, which is significantly longer than those reported for dinuclear Ca–Ca distances of 3.860(2) Å and 3.891(4) Å,^{16,17} whereas the two metal atoms bridged by O3 and O4 of the same carboxylate (*anti-anti* mode) are 6.616(1) Å (the length of the *a*-axis). The topology of the six-connected metal centers is assigned to the α -Po structure (Figure 7). All Ca–O (carboxylate) atomic distances (2.295(2)–2.604(3) Å) in **1**, **2**, and **3** fall within the normal range of previously reported values.¹⁸ Three different coordination modes are found for H₂pdc²⁻ in **1**, **2**, and **3** (see Scheme 2a, b, c), and the connectivity numbers increase from

(16) Ueyma, N.; Takeda, J.; Yamada, Y.; Onoda, A.; Okamura, T. *Inorg. Chem.* **1999**, *38*, 475.

(17) Bahl, A. M.; Krishnaswamy, S.; Massand, N. G.; Burkey, D. J.; Hanusa, T. P. *Inorg. Chem.* **1997**, *36*, 5413.

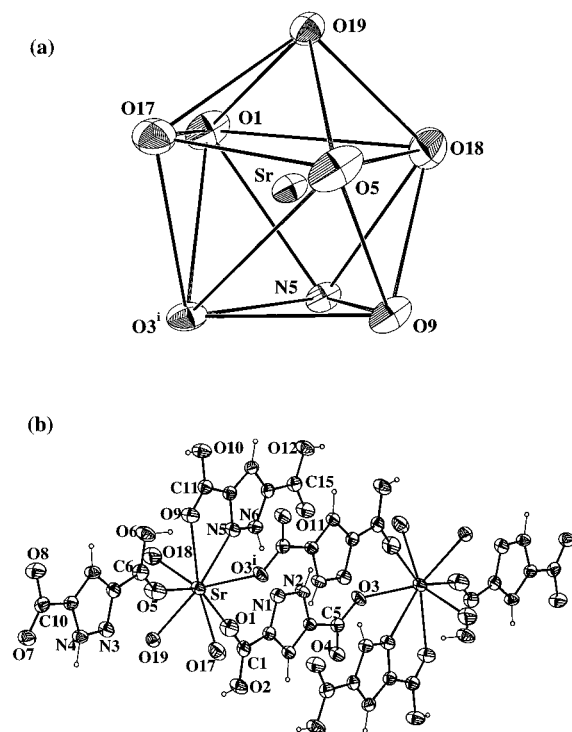


Figure 8. (a) Coordination polyhedron around the Sr metal in **4**. (b) ORTEP drawing of the dimer molecule in **4** with numbering scheme, 50% probability of ellipsoids. The H atoms from the coordinated water are omitted for clarity.

μ_3 , μ_4 , up to μ_6 with increasing pH value. This finding reveals that H₂pdc²⁻, like other similar ligands,¹⁹ tends to form five-member chelating rings at low pH values. When a basic species (a reagent or a solvent) is introduced to the reaction, the carboxylate groups tend to form four-member chelating rings with the metal centers.

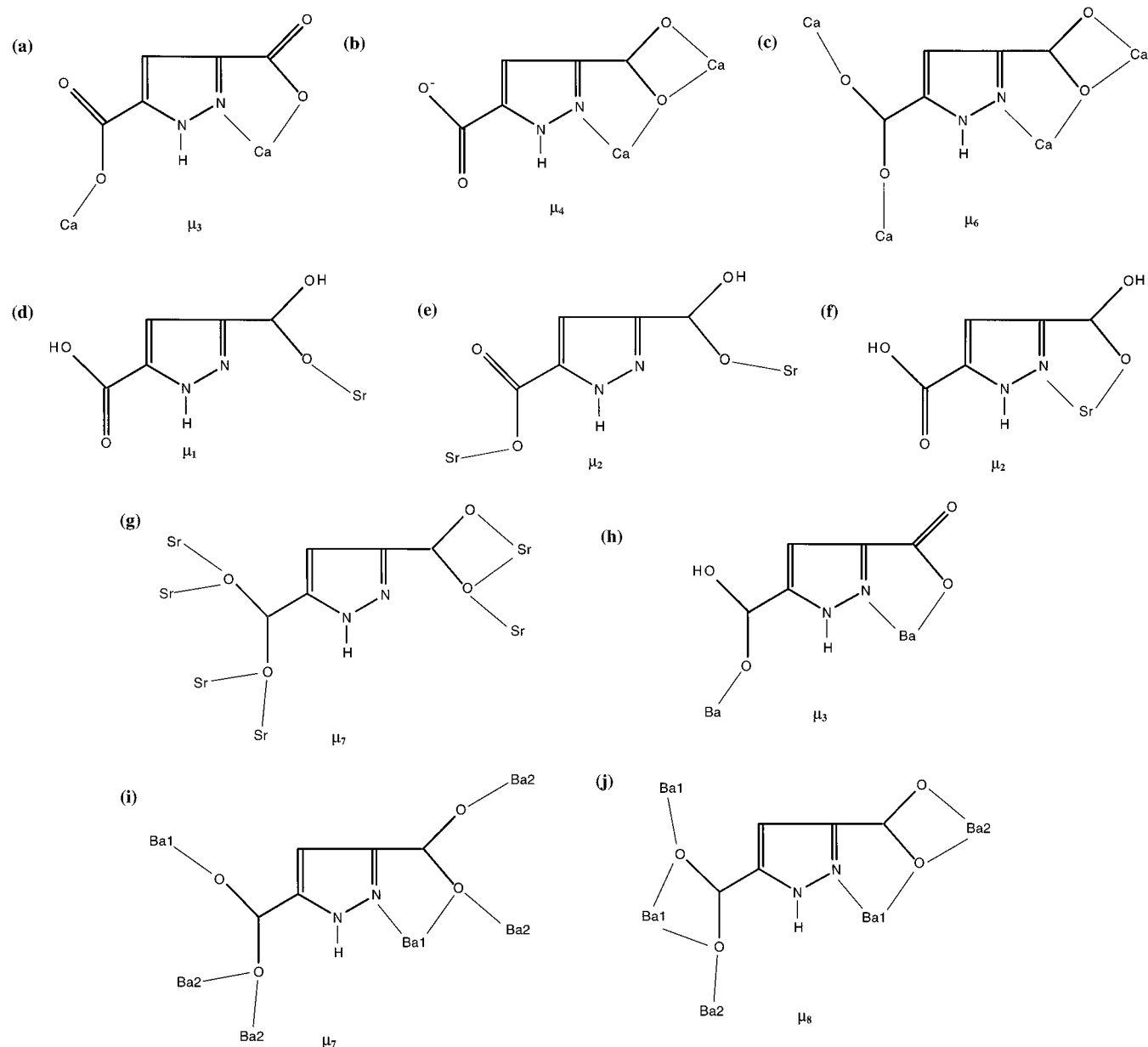
Attempts to synthesize analogous structures with an alkaline-earth metal of larger radius, such as strontium, with the same experimental procedures were not successful. Rather, crystals of **4** were grown from a strontium perchlorate solution at low pH values. The unit cell of **4** consists of a [Sr(H₃pdc)(H₂pdc)₂(H₂O)₃]₂ dimer, two uncoordinated H₃pdc, and four lattice water. An ORTEP drawing of this dimer is shown in Figure 8b. Selected bond lengths and angles are listed in Table 3. The coordination environment of strontium metal can be best described as a trigonal dodecahedron (Figure 8a). The coordination sphere consists of three monodentate carboxyl oxygen atoms (O1, O3¹, O5), each from a separate H₂pdc⁻ ligand, a nitrogen, and an oxygen from the five-member chelating ring (O9, N5) of the H₃pdc ligand. The remaining positions are occupied by three coordinated water molecules (O17w, O18w, O19w). The Sr atoms form pairs through two bridging H₂pdc⁻ ligands which bond to the two metal centers via the two monodentate carboxylate oxygen atoms to give rise to a [2+2] metallomacrocyclic (Figure 9).²⁰ The distance between the two Sr(II) ions is 9.694(5) Å. It is interesting to note that the pyrazole ring of

(18) Costa, J.; Delgado, R.; Drew, M. G. B.; Felix, V.; Henriques, R. T.; Waerenborgh, J. C. *J. Chem. Soc., Dalton Trans.* **1999**, 3253. (b) Sahbari, J. J.; Olmstead, M. M. *Acta Crystallogr.* **1985**, *C41*, 360. (c) van der Sluis, P.; Schouten, A.; Spek, A. L. *Acta Crystallogr.* **1987**, *C43*, 1922.

(19) Barnett, B. L.; Uchtman, V. A. *Inorg. Chem.* **1979**, *18*, 2674. (b) Hundal, G.; Martinez-RiPoll, M.; Hundal, M. S. *Acta Crystallogr.* **1995**, *C51*, 1788.

(20) Bilyk, A.; Harding, M. M. *Chem. Commun.* **1995**, 1679.

Scheme 2



one bridging $\text{H}_2\text{pdc}^{2-}$ ligand is right above the pyrazole ring of a chelating H_3pdc while the pyrazole ring of the second bridging $\text{H}_2\text{pdc}^{2-}$ ligand is right below the pyrazole ring of the second chelating H_3pdc . The two pyrazole rings in each pair are approximately parallel with respect to each other with an average distance of 3.71 Å which is likely to be subject to a π - π interaction.²¹ The dicarboxylate ligands have three coordination modes in this compound, μ_1 , and two μ_2 , as drawn in Scheme 2d, e, and f. There is a strong hydrogen bond between the dimer and uncoordinated H_3pdc molecule ($\text{O}8-\text{H}3\cdots\text{O}13 = 2.447(4)$ Å). Another strong hydrogen bond exists between the dimers themselves ($\text{O}10-\text{H}4\cdots\text{O}4 = 2.488(4)$ Å), resulting in a one-dimensional chain. Further hydrogen-bonding among the chains leads to a three-dimension H-bonded network. When $\text{Sr}(\text{OH})_2$ was used as a precursor, or EtN_3 was added to the reaction to increase the pH value, structure **5** was isolated. Single-crystal X-ray diffraction revealed that **5** crystallizes in a three-

dimensional network structure. Quite differently from the coordination environments in **1**–**4**, the metals in **5** are nine-coordinated and surrounded entirely by oxygen atoms, of which seven are from Hpdc^{2-} and two from H_2O , resulting in a singly capped square antiprism (Figure 10). Important bond lengths and angles are listed in Table 3. Illustrated in Figure 11 is a view of **5** along the c axis. All strontium atoms are located in the bc planes and form distorted square lattices (Figure 12) with Sr–Sr distances of 4.077, 4.401, 4.401 and 4.448 Å, respectively, for the four sides of the “square”. The separation between the neighboring planes is 9.213 Å ($=a$). The metals in the neighboring planes are bridged by Hpdc^{2-} via its two carboxylate groups in tridentate (η^1, η^2) and tetradentate (η^2, η^2) fashion, respectively (see Scheme 2g), to result in a three-dimensional structure, as plotted in Figure 11. This coordination mode of Hpdc^{2-} is quite rare.²²

(21) Hunter, C. A.; *Angew. Chem., Int. Ed. Engl.* **1993**, *32*, 1584. (b) Hartshorn, C. M.; Steel, P. J. *Inorg. Chem.* **1996**, *35*, 6902.

(22) Christensen, A. N.; Hazell, R. G. *Acta Chem. Scand.* **1998**, *52*, 508. (b) Price, D. J.; Powell, A. K.; Wood, P. T. *Polyhedron* **1999**, *18*, 2499. (c) Helems, R.; Cole, L. B.; Holt, E. M. *Inorg. Chim. Acta* **1988**, *152*, 9.

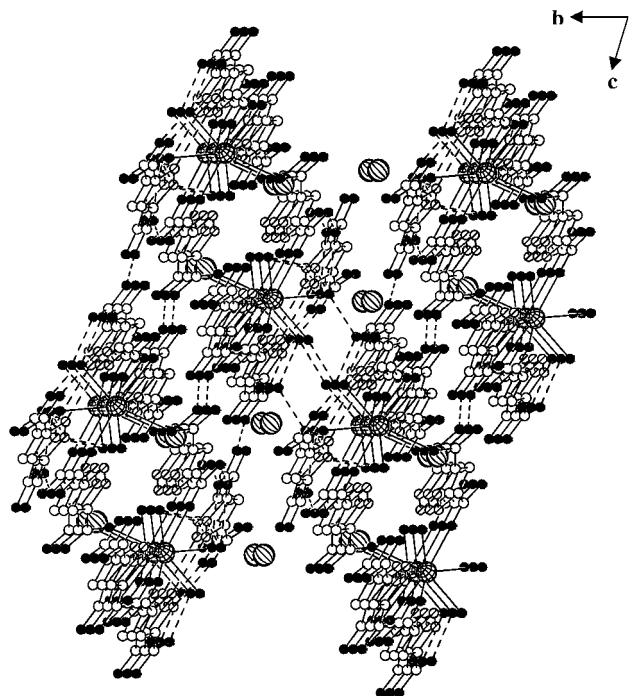


Figure 9. Molecular parking in **4**, H-bonds among the dimers are in dashed lines. A similar labeling scheme to that of Figure 2 is used here. Lattice water molecules are shown as large shaded circles. The H atoms are omitted for clarity.

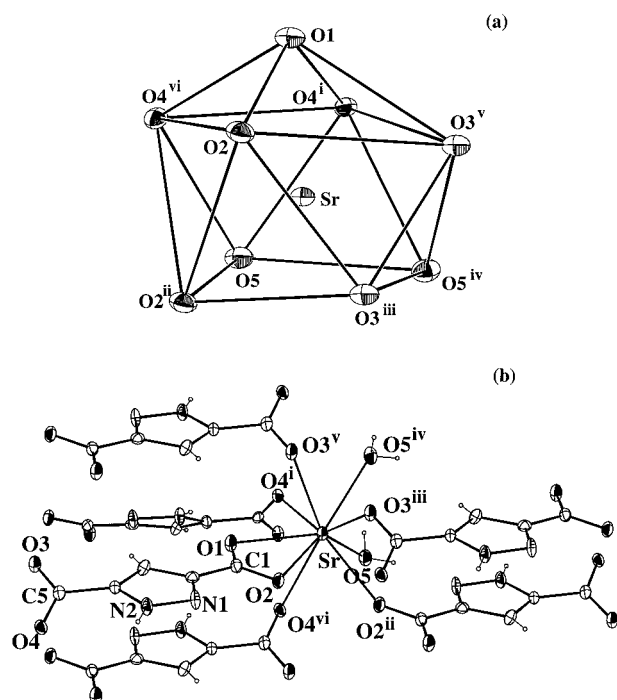


Figure 10. (a) Coordination polyhedron around the Sr metal in **5**. (b) Coordination environment of **5** (ORTEP drawing with 50% probability of ellipsoids).

With barium, the Group 2 metal with largest radius of our choice (calcium, strontium, and barium), reactions similar to those for compound **1** yielded one-dimensional structure **6**. The Ba(II) located on an inversion center is coordinated by 10 atoms to form a trigonal hexadecahedron (Figure 13). Among the four H_2pdc^- ligands, two bond to the metal center via a chelating mode through a carboxylate oxygen (O1) and its adjacent nitrogen atom (N1) in the pyrazole ring and the other two

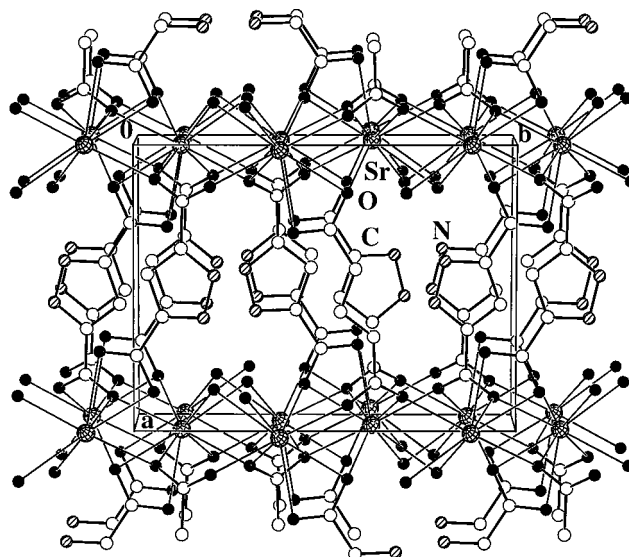


Figure 11. View of the three-dimensional structure of **5** along the *c*-axis. The Hpdc^{2-} groups are approximately vertical with respect to the metal (*bc*) plane. A similar labeling scheme to that of Figure 2 is used here. The H atoms are omitted for clarity.

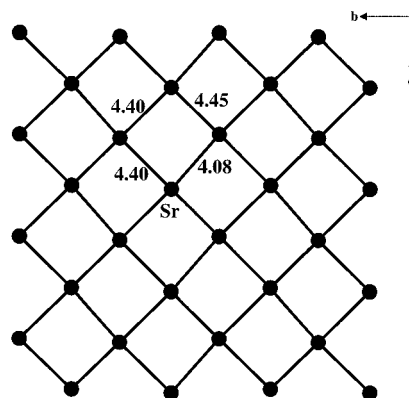


Figure 12. View of the *bc* plane showing the square lattice of the metal atoms in **5**. The shortest Sr–Sr distances are indicated in the figure.

through a monodentate carboxylate group (O3). The remaining sites are occupied by oxygen atoms (O5^w, O6^w, O5^w, O6^w) from coordinated water. The metals are interconnected by two H_2pdc^- to form a ribbon running along the [101] direction, as shown in Figure 14a. The bonding pattern of each dicarboxylate in the chain is nearly identical to that in **1**. The only difference is that there are two bridging dicarboxylate ligands between each pair of metals in **6**, while in **1** the neighboring metals are bridged by a single dicarboxylate ligand. The difference between the coordination modes of Hpdc^{2-} in **1** and H_2pdc^- in **6** is that the latter has one more unde protonated hydrogen in the carboxylate group (Scheme 2h) that is engaged in a strong intrachain hydrogen bond (O4–H1...O1, 2.499(6) Å). Figure 14b illustrates the ribbons that are hydrogen-bonded via coordinated water and dicarboxylate molecules, which leads to a three-dimensional H-bonding structure. The lattice water molecules are located in the channels resulted from the H-bonding network. The selected bond lengths and angles are given in Table 6. The H-bonding parameters are given in Table 6. When the pH value was changed by adding a basic solvent, or by using a basic precursor, the three-dimensional structure **7** based on the barium ion was isolated. Figure 15 shows the coordination environment of two independent barium ions. Ba1

Table 7. Metal Coordination Number (CN), Reaction pH, Ligand Connectivity (μ), and Structure Dimensionality (D) of M–pdc Compounds

compound	CN	pH	μ	D	reference
[Ca(Hpdc)(H ₂ O) ₄]·2H ₂ O	7	2.5	3	1	this work
[Ca(Hpdc)(H ₂ O) ₄]·H ₂ O	8	2.5	4	1	this work
[Ca(Hpdc)(H ₂ O)]	7	6.0	6	3	this work
[Sr(H ₃ pdc)(H ₂ pdc) ₂ (H ₂ O) ₃] ₂ ·2(H ₃ pdc)·4H ₂ O	8	2.5	1, 2	0 (dimer)	this work
[Sr(Hpdc)(H ₂ O)]	9	4	7	3	this work
[Ba(H ₂ pdc) ₂ (H ₂ O) ₄]·2H ₂ O	10	2.5	3	1	this work
[Ba(Hpdc)(H ₂ O)]	9, 10	5	7, 8	3	this work
[Cd(Hpdc)H ₂ O]	7	4	6	3	6c
[Cd ₃ (pdc) ₂ (H ₂ O) ₂]	6	6	7	3	6c
[Ln ₂ (Hpdc) ₃ (H ₂ O) ₄]·2H ₂ O, Ln = La, Ce, Eu	9	2.5	4, 5	3	6b
[Eu ₂ (Hpdc) ₃ (H ₂ O) ₆]	8	2.5	2, 4	2 (bilayer)	6b
[Er ₂ (Hpdc) ₃ (H ₂ O) ₆]	8	5	2, 4	2 (bilayer)	6b
[Lu(Hpdc)(H ₂ pdc)(H ₂ O) ₂]	8	2.5	2, 3	2 (single layer)	6b
[Er(Hpdc)(H ₂ pdc)(H ₂ O) ₂]	8	1	2, 3	2 (single layer)	6b

Thermogravimetric and FT-IR Analyses. Three 3D compounds (**3**, **5**, **7**) were examined by TGA in nitrogen gas to investigate their thermal decomposition and adsorption. The drastically different decomposition behavior of these compounds has been observed. When heating to 250 °C, calcium compound **1** began to lose weight and decompose gradually with increasing temperature, the TGA curve does not show any clear step. On the contrary, the first step in strontium compound **5** (300–440 °C) and barium compound **7** (250–400 °C) correspond to the loss of one water in **5** (7.1%, Cal. 6.9%) and one water in **7** (5.8%, Cal. 5.8%). A comparison of the PXRD patterns of the residues, from which one water per formula has been removed, and their corresponding original materials **5** and **7** show that different phases have resulted. After reintroducing water to these dehydrated materials over several hours, the PXRD spectra of the resultant solids reveal new patterns different from both the original solids and the dehydrated products.

The FT-IR spectra show strong peaks around the 1600–1400 cm⁻¹, which is characteristic of the expected adsorption for carboxylate vibration. The stretching vibrations around 3500 cm⁻¹ in all spectra are attributed to secondary aromatic amine (V = N–H). This confirms with the observations from the single-crystal X-ray analysis that all hydrogen atoms attached to pyrazole nitrogen are not deprotonated. The strong peaks are around 1655–1400 cm⁻¹, which is characteristic of the expected adsorption for asymmetric and symmetric vibrations for uni- and bidentate carboxylate groups.²⁴

Concluding Remarks

Investigation of the effect of pH in carboxylic acid systems is of particular importance because it helps us to understand the correlation between the reaction acidity and the structure dimensionality. As a comparison, metal coordination number, pH level, and dimensionality of several metal–pdc structures are listed in Table 7. Our previous work on 3,5-pyrazoledicarboxylic acid as a multiple dentate ligand has shown that this ligand readily reacts with rare-earth, transition, and post-transition metal ions to yield versatile structures. By adjusting the pH level desired products may be isolated and purified.^{1,6b–c} In this work, we have extended our investigation to systems containing alkaline-earth metals. Although Group 2 metals belong to hard acids similar to rare-earth metals according to soft–hard theory, they have a wider range of radii than that of lanthanide series resulting from *lanthanide contraction*. The acidity levels of the reactions have been adjusted not only by adding basic solvents but also by introducing basic precursors,

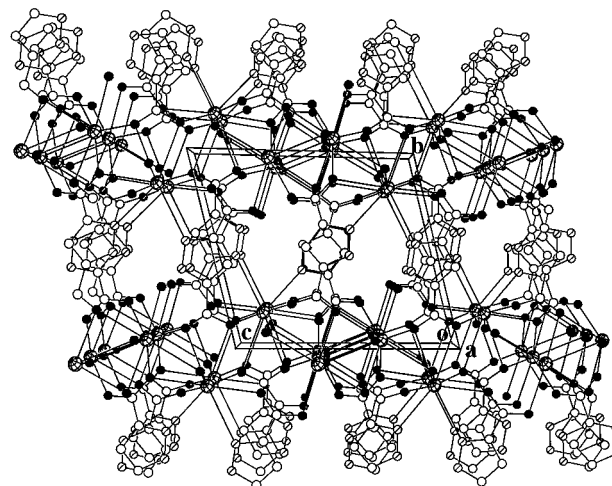
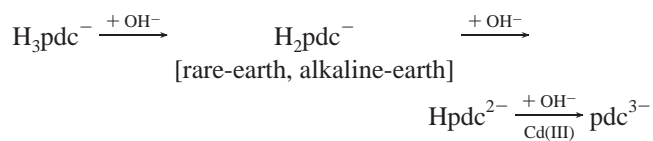


Figure 16. View of the three-dimensional structure of **7** along the *a*-axis. The Hpdc²⁻ groups as pillar molecules bridge the metal layers comprised of Ba1 and Ba2. A similar labeling scheme to that of Figure 2 is used here. The H atoms are omitted for clarity.

such as Ca(OH)₂, Sr(OH)₂, and Ba(OH)₂. Seven crystal structures, ranging from low-dimension to high-dimension, have been synthesized and analyzed. The coordination number increases from 7, 8 (calcium) to 8, 9 (strontium) and finally to 9, 10 (barium) as a result of increase in ionic radii. However, it is quite clear that the metal coordination number in these reactions is not the determining factor for high dimensionality. For example, low dimensional structures form for all three metal ions (Ca, Sr, and Ba) with high coordination numbers 8 (**2**, **4**) and 9 (**6**). The reaction acidity, however, does play a crucial role in the structure formation. In general, increasing pH leads to higher connectivity (μ) of the ligands and ultimately structures of higher dimensions. For the three calcium compounds, the connectivity varies from μ_3 and μ_4 for the one-dimensional structures **1** and **2**, respectively, to μ_6 for the three-dimensional structure **3**. The two strontium compounds have a μ_1 and two μ_2 connectivity in **4** (a [2+2] dimer molecule) and a μ_7 in **5** (three-dimensional structure). In the case of the two barium compounds, the μ_3 connectivity yields a one-dimensional structure **6**, whereas μ_7 and μ_8 give rise to a three-dimensional structure **7**. It is also noted that at lower pH level, alkaline-earth metal elements show a high tendency to coordinate with water molecules, resulting in a high water-to-metal ratio, thus limiting their ability to form structures of higher dimensionality as rare-earth metals and cadmium. The comparisons among different metal–pdc species also show that the hydrogen atom attached to the pyrazole ring of the dicarboxylate cannot be deprotonated in either rare-earth or alkaline-earth metal com-

(24) Robinson, S. D.; Utey, M. F. *J. Chem. Soc., Dalton Trans.* **1973**, 1914.

pounds. Such a deprotonation can only take place with the softer cadmium metal. The relation between the pH value and the coordination state of the ligand is illustrated below.



Acknowledgment. We thank the National Science Foundation for its generous support via Grant DMR-9553066 and the REU supplemental funds.

Supporting Information Available: Four X-ray crystallographic files, in CIF format. This material is available free of charge via the Internet at <http://pubs.acs.org>.

IC001012O